

Harmonic generation with temporally focused ultrashort pulses

Dan Oron and Yaron Silberberg

Department of Physics of Complex Systems, The Weizmann Institute of Science, Rehovot 76100, Israel

Received April 19, 2005; revised manuscript received July 10, 2005; accepted June 28, 2005

The properties of harmonic generation with temporally focused ultrashort pulses are explored both theoretically and experimentally. Analyzing the phase-matching conditions for harmonic generation we find a correspondence between temporal focusing and spatial focusing along one dimension. In particular, temporally focused pulses experience a π phase shift in passing through the temporal focus, similar to the Guoy phase shift experienced by spatially focused beams. This correspondence is confirmed by measurements of third-harmonic generation induced by temporally focused pulses. © 2005 Optical Society of America

OCIS codes: 110.6880, 180.5810, 190.4160, 190.7110.

1. INTRODUCTION

Temporal focusing of ultrashort pulses has recently been suggested as a mechanism to perform depth-resolved multiphoton microscopy completely without scanning.¹ In another realization, temporal focusing can be used in conjunction with spatial focusing along a single spatial axis to improve the depth resolution (and the signal-to-background ratio) in line-scanning multiphoton microscopy.^{2,3} In short, the realization of temporal focusing relies on the Fermat principle, stipulating that, in an imaging system, the pulse duration at the image is equal to its duration at the object. In practice, if the ultrashort pulse impinges upon a plane scatter, be it a coherent one (i.e., a grating) or an incoherent one (a diffuser), which is imaged onto the sample, the pulse duration can be significantly stretched in regions other than the image plane. As a result, the multiphoton signal is generated efficiently only at the image plane, which is equivalent to a temporal focal plane of the imaging system.

An analysis of the illumination pulse duration as a function of the spatial coordinates is sufficient to determine the depth of focus and the generated signal when the excited multiphoton is an incoherent one, such as multiphoton fluorescence,^{4,5} as in Refs. 1–3. This is, however, insufficient when we are considering a coherent multiphoton signal, such as harmonic generation^{6–11} or coherent anti-Stokes Raman scattering.^{12–15} In the latter case, the spatial dependence of the phase of the scattered multiphoton light is of utmost importance for determination of the overall signal. In Section 2 we formulate an analytic solution for harmonic generation by temporally focused pulses and show that under certain conditions this solution is similar to that of harmonic generation by

a cylindrically focused Gaussian beam.¹⁶ In Section 3 we proceed to show this correspondence experimentally, establishing the applicability of temporal focusing to coherent multiphoton microscopy applications.

2. MATHEMATICAL FORMULATION OF HARMONIC GENERATION WITH TEMPORALLY FOCUSED PULSES

In the following we consider the case of an asymmetric $4f$ pulse shaper, as shown in Fig. 1. The setup consists of a high-magnification telescope comprised of an achromatic lens and a microscope objective, and a grating, placed at the focal plane of the achromatic lens and aligned perpendicular its optical axis so that the entire illuminated area indeed lies at the focal plane. The grating is illuminated by a plane ultrashort pulse at an angle such that the central frequency of the illumination pulse ω_0 is diffracted toward the optical axis of the achromatic lens. The different frequency components of the pulse thus emanate as plane waves from the microscope objective, each propagating at a different angle. Note that this is somewhat different from the case described by Zhu *et al.*,³ where the achromatic lens and the microscope objective do not form a telescope. In the paraxial approximation, after passing through the objective lens, we obtain

$$k(\omega) = k_\omega \cos(\theta_\omega) \hat{z} + k_\omega \sin(\theta_\omega) \hat{x} \approx k_\omega (1 - \theta_\omega^2/2) \hat{z} + k_\omega \theta_\omega \hat{x}. \quad (1)$$

Assuming that the angular spread of the pulse spectrum by the grating is linear (corresponding to a pulse duration much longer than a single cycle), we can write $\theta_\omega = P(\omega - \omega_0) = P\delta$.

Utilizing this, the electric field can be written as a Fourier integral:

$$E(x,z,t) = \int d\omega g(\omega) \exp[i\mathbf{k}(\omega) \cdot \mathbf{r} - i\omega t] \\ = \int d\omega g(\omega) \exp[ik_\omega z(1 - P^2 \delta^2/2) + ik_\omega x P \delta - i\omega t], \quad (2)$$

where the pulse spectral amplitude is $g(\omega)$. Assuming a Gaussian form for $g(\omega)$, substituting $k_\omega = k_0 + \delta/c$ (neglecting dispersion) and taking the carrier frequency out of the integral, we obtain

$$E(x,z,t) = g_1 \exp[i(k_0 z - \omega_0 t)] \int d\delta \exp(-\delta^2/\Delta^2) \exp[i(\delta/c \\ - k_0 P^2 \delta^2/2 - P^2 \delta^3/2c)z + i(k_0 P \delta + P \delta^2/c)x - i\delta t], \quad (3)$$

where Δ is the spectral bandwidth of the excitation pulse. Again, for pulse durations much longer than a single cycle, $\delta/c \ll k_0$ so the last term in the z exponent as well as the last term in the x exponent can be dropped. Overall, the integral is of the form $\int dx \exp(-Ax^2) \exp[ix(t-t_0)]$, with

$$A = \frac{1}{\Delta^2} (1 + ik_0 \Delta^2 P^2/2z); \quad t_0 = (k_0 P x - z/c). \quad (4)$$

Defining the nondimensional z coordinate $\xi = k_0 P^2 \Delta^2 z/2$, we can rewrite A as $A = 1/\Delta^2 (1 + i\xi)$.

Performing the Fourier-transform operation we finally obtain

$$E(x,z,t) = \exp[i(k_0 z - \omega_0 t)] \frac{g_1 \Delta \sqrt{\pi}}{\sqrt{1 + i\xi}} \exp\left[\frac{\Delta^2 (t - t_0)^2}{4(1 + i\xi)}\right]. \quad (5)$$

As expected from a temporally focused beam,^{1,3} the exponential term in Eq. (5) describes a pulse with a Gaussian temporal profile, where the Gaussian width is minimal at $z=0$. The x dependence of t_0 describes a spatial focus that moves along the x coordinate at a velocity $v = (k_0 P)^{-1}$. Note that this velocity differs by a factor of

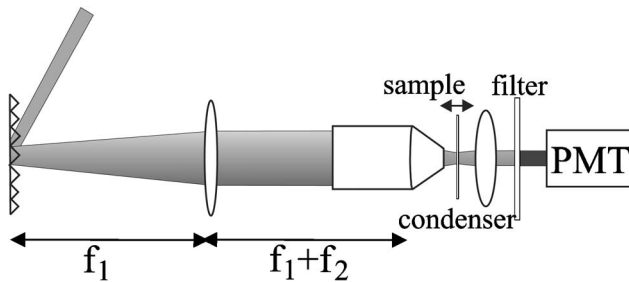


Fig. 1. Experimental setup of third-harmonic generation (THG) by temporally focused beams. The input beam impinges upon a grating, aligned perpendicular to the optic axis of the microscope. The grating is imaged through a high-magnification telescope, comprised of a cylindrical lens and the microscope objective, on the sample. The integrated THG signal is collected in the forward direction and measured by a photomultiplier tube (PMT).

$(1/\omega_0)(d\omega/d\theta)$ than the speed of light and, under conditions typical of multiphoton microscopy (i.e., strong magnifications), is typically much smaller than the speed of light. The coefficient represents a field amplitude that for $|z| \gg 0$ decreases as $\sqrt{|z|}$, as is the case for a cylindrically focused Gaussian beam.

It is indeed instructive to compare the solution of Eq. (5) with the field amplitude of a continuous-wave cylindrically focused Gaussian beam:

$$E(x,z) = \exp[i(k_0 z - \omega_0 t)] \frac{A_1}{\sqrt{1 + i\xi}} \exp\left[-\frac{x^2}{w_0^2(1 + i\xi)}\right], \quad (6)$$

where $\xi = 2z/b$ is the dimensionless longitudinal coordinate defined in terms of the confocal parameter $b = kw_0^2$, and w_0 is the beam waist.¹⁶ As can be easily seen, the parameter ξ in Eq. (5) is equivalent to ξ in Eq. (6). This implies that the confocal parameter b be replaced with $b' = (k_0 \Delta^2 P^2)^{-1}/4$. Rephrasing this, the expression $2/(kw_0)$ in Eq. (6) is replaced by ΔP in Eq. (5). This is not surprising, since both expressions simply represent the far-field beam divergence. In a practical microscope system this is the parameter that determines both the depth resolution and the axial resolution, which is limited by the numerical aperture of the objective lens.

As a matter of fact, this correspondence is to be expected when we take the time-domain picture of temporal focusing by the setup described in Fig. 1. As discussed by Oron *et al.*,¹ the incoming pulse, impinging upon the grating at an angle, does not illuminate the entire grating simultaneously, but rather scans across it. The temporal focus, being just the image of the illuminated grating, similarly scans across the sample. Naïvely, this is just like when line scanning is applied, only that the full frame is scanned within a few picoseconds by the traveling pulse itself.

We now try to extend this analogy to the solution of the harmonic-generated wave. The analytical solution of the harmonic wave generated by a focused Gaussian beam is based on the fact that the functional form of the fundamental electric field distribution raised to the q th power is similar to that of a focused harmonic Gaussian beam. Raising Eq. (5) to the q th power, we obtain

$$[E(x,z,t)]^q = \exp[i(qk_0 z - q\omega_0 t)] \\ \times \frac{\Delta^q \pi^{q/2}}{(1 + i\xi)^{(q/2)}} \exp\left[\frac{q\Delta^2 (t - t_0)^2}{4(1 + i\xi)}\right]. \quad (7)$$

Looking at the exponent, this would represent a temporally focused harmonic beam provided that for the harmonic beam one would obtain $t'_0 = t_0$, $\xi' = \xi$, $\Delta' = \sqrt{q}\Delta$. This is realized only if $k_q = qk_0$, $\omega_q = q\omega_0$, $P_q = P/q$. This means that the harmonic wave is strictly a similar temporally focused beam only in the case of perfect phase matching, as is also the case for focused Gaussian beams (where it is assumed that $b = kw_0^2$ is the same for both the fundamental and the harmonic and $w_0 \rightarrow w_0/\sqrt{q}$ ^{16,17}). In practice this approximation is reasonable when the phase mismatch fulfills $k_q - qk_0 \ll k_q$. Since this condition is practi-

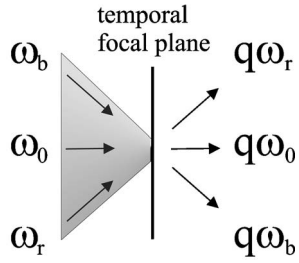


Fig. 2. Geometry of the temporally focused beam and the resulting harmonic beam. The fundamental beam is comprised of plane waves at different frequencies propagating at different angles. At the temporal focal plane, all frequencies constructively interfere to generate a focal spot moving along the x axis. The generated harmonic is similarly a temporally focused beam, implying that each harmonic frequency $q\omega$ copropagates with the fundamental ω .

cally fulfilled in most cases, we can, in analogy with the spatial solution, make the ansatz

$$E_q(x, z, t) = C(z) \exp[i(k_q z - q\omega_0 t)] \frac{\Delta \sqrt{q\pi}}{\sqrt{1+i\xi}} \exp\left[\frac{q\Delta^2(t-t_0)^2}{4(1+i\xi)}\right], \quad (8)$$

where $C(z)$ is a slowly varying amplitude for the harmonic wave. This means that the harmonic beam is a temporally focused one, with an intensity that varies only along the z axis. As is shown in Fig. 2, this reflects the fact that the different spectral components of the harmonic signal propagate at different directions, where the harmonic frequency $q\omega$ copropagates with the fundamental frequency ω . In wave-vector space this phenomenon can be readily understood since for all frequency combinations where $\sum_{i=1,q} \omega_i = q\omega$, the sum of wave vectors in the direction parallel to k_ω is just qk_ω (in the paraxial approximation) while the sum of wave vectors in the perpendicular direction is proportional to $\sum_{i=1,q} (\omega_i - \omega) = 0$, which identically vanishes (neglecting dispersion).

Performing the integration for the coefficient $C(z)$ in Eq. (8), we end up with a solution of the form (keeping the phase mismatch in the coefficient):

$$C(z) \propto \int dz \frac{\exp[i(k_q - qk_0)]}{(1+i\xi)^{(q-1)/2}}, \quad (9)$$

which is similar to the solution for a cylindrically focused Gaussian beam. Since this solution is entirely two-dimensional, combining spatial focusing along the y axis with temporal focusing, as in Refs. 2 and 3, would simply result in modification of relation (9):

$$C(z) \propto \int dz \frac{\exp[i(k_q - qk_0)]}{(1+i\xi)^{(q-1)/2} (1+i\zeta)^{(q-1)/2}}. \quad (10)$$

The derivation here is similar to the one of spatial focusing along two axes, where the x and y variables can be separated and each contributes a $(1+i\zeta)^{(q-1)/2}$ in the denominator.

Following this derivation we obtain the result that, in the specific case of third-harmonic generation (THG) (i.e., $q=3$), no signal would arise from a bulk medium exhibiting normal dispersion. Similar to both cases of spatial fo-

cusings, either along one or two spatial axes, a signal would be observed only from interfaces and small inclusions, on the scale of the temporal confocal parameter b' .

3. EXPERIMENTAL MEASUREMENT OF THE CROSS-SECTIONING PROPERTIES OF THIRD-HARMONIC GENERATION BY TEMPORALLY FOCUSED PULSES

In the following experiment we show quantitatively the correspondence between temporal focusing and spatial focusing along one spatial dimension by comparing the cross-sectioning properties of THG for the two cases.

The laser source used in the experiments is an optical parametric oscillator delivering 100 fs pulses at $1.5 \mu\text{m}$ with an energy of ~ 2 nJ at a repetition rate of 80 MHz (Spectra-Physics OPAL). In the experiments a 600 line/mm grating (blazed for 1600 nm) was used, corresponding to near-grazing-incidence illumination. The cylindrical telescope lens had a focal length of 25 cm. To decrease the illuminated area for the temporally focused beam, a $4\times$ cylindrical telescope was used to shrink the beam size in the horizontal direction. Because of the large angle of incidence, this resulted in a nearly circular 3 mm illuminated spot on the grating. Laser light was focused into the sample using an 0.85 numerical aperture objective lens. THG light was collected by a condenser lens, filtered by a bandpass filter at 500 nm, and measured by a photomultiplier tube and a lock-in amplifier. Because the THG signal rapidly decreases with an increased illumination area, we chose to compare the depth resolution obtained by point illumination with that achieved by combined temporal focusing and spatial focusing along one dimension, as in Refs. 2 and 3.

Measurements of the depth resolution were performed by using a glass coverslip perpendicular to the microscope axis and mounted on a piezoelectric stage as a sample.

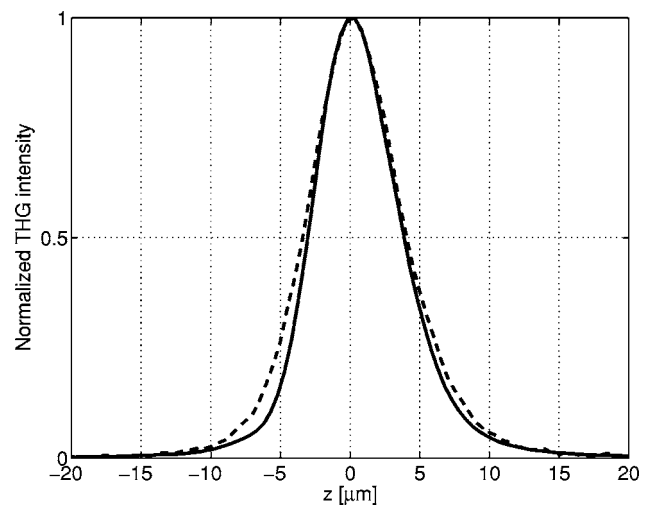


Fig. 3. Comparison of the cross-sectioning capabilities of THG excited by single point illumination by spatial focusing along two spatial axes (solid curve) and line illumination by combined temporal focusing and spatial focusing along a single spatial axis (dashed curve). As can be seen, the two cases result in an identical depth resolution, as expected following the analysis of Section 2.

For the case of a temporally focused beam, the THG signal from the entire sample was collected and integrated.

The results of a z scan through the sample are plotted for the two cases in Fig. 3. As can be seen, THG indeed arises only from the glass–air interface and vanishes when the beams are focused within the bulk. The cross-sectioning properties of both focusing geometries are practically identical, in correspondence with the predictions of relation (10).

4. CONCLUSION

When introducing a new illumination geometry to coherent multiphoton microscopy applications, care has to be taken to take into account phase-matching considerations. The new technique of temporal focusing has been utilized for effective multipoint illumination only in incoherent multiphoton microscopy, based on multiphoton fluorescence. Here we derive an analytical theory applicable for harmonic generation microscopy with temporally focused illumination and show that the analogy between temporal focusing and spatial focusing along one axis holds even for coherent processes. In particular, temporally focused beams experience an analog of the Guoy phase shift when passing through the temporal focal plane. These results indicate that space-multiplexed multiphoton microscopy based on temporal focusing can also be readily applied to coherent processes.

While harmonic generation with temporally focused beams is in many cases analogous to the spatial focusing case, there are still significant differences that arise from the different excitation geometry. In general, the spectral frequency assumes the role typically taken by the spatial frequency. The generated harmonic signal is, by itself, a temporally focused pulse. Thus the different frequency components of the generated harmonic signal are emitted at different directions. As a result, just as an arbitrarily shaped scatterer influences the wave-vector distribution of the outgoing signal,¹⁸ for temporally focused illumination it would affect the spectrum of the scattered signal.

The peculiar properties of coherent multiphoton processes excited by temporally focused pulses can be combined with Fourier-transform pulse-shaping techniques¹⁹ to enable enhanced spatial control of the multiphoton excitation volume. In practice, since the optical setup is of an asymmetric $4f$ pulse shaper, this merely requires the inclusion of a spatial light modulator in front of the objective lens. For example, by polarization pulse shaping, one can generate a spatially varying polarization in the vicinity of the temporal focal plane. Such effects could be used to distinguish scatterers and absorbers with polarization-dependent properties.

ACKNOWLEDGMENTS

The authors thank E. Tal for helpful discussions. Financial support from the Israel Science Foundation and from the Horowitz Foundation is gratefully acknowledged.

REFERENCES

1. D. Oron, E. Tal, and Y. Silberberg, "Scanningless depth-resolved microscopy," *Opt. Express* **13**, 1468–1476 (2005).
2. E. Tal, D. Oron, and Y. Silberberg, "Improved depth resolution in video-rate line-scanning multiphoton microscopy using temporal focusing," *Opt. Lett.* **30**, 1686–1688 (2005).
3. G. Zhu, J. van Howe, M. Durst, W. Zipfel, and C. Xu, "Simultaneous spatial and temporal focusing of ultrashort pulses," *Opt. Express* **13**, 2153–2159 (2005).
4. W. Denk, J. H. Stricker, and W. W. Webb, "Two-photon laser scanning fluorescence microscopy," *Science* **248**, 73–76 (1990).
5. S. Maiti, J. B. Shear, R. M. Williams, W. R. Zipfel, and W. W. Webb, "Measuring serotonin distribution in live cells with three-photon excitation," *Science* **275**, 530–532 (1997).
6. G. Peleg, A. Lewis, O. Bouevitch, L. Loew, D. Parnas, and M. Linial, "Gigantic optical non-linearities from nanoparticle-enhanced molecular probes with potential for selectively imaging the structure and physiology of nanometric regions in cellular systems," *Bioimaging* **4**, 215–224 (1996).
7. Y. Barad, H. Eisenberg, M. Horowitz, and Y. Silberberg, "Nonlinear scanning laser microscopy by third harmonic generation," *Appl. Phys. Lett.* **70**, 922–924 (1997).
8. M. Muller, J. Squier, K. R. Wilson, and G. J. Brakenhoff, "3D-microscopy of transparent objects using third-harmonic generation," *J. Microsc.* **191**, 266–274 (1998).
9. J. A. Squier, M. Muller, G. J. Brakenhoff, and K. R. Wilson, "Third harmonic generation microscopy," *Opt. Express* **3**, 315–324 (1998).
10. D. Yelin and Y. Silberberg, "Laser scanning third-harmonic-generation microscopy in biology," *Opt. Express* **5**, 169–175 (1999).
11. D. Yelin and Y. Silberberg, "Third-harmonic microscopy in biology," *Microscopy and Analysis* **80**, 15–18 (2000).
12. A. Zumbusch, G. R. Holtom, and X. S. Xie, "Three-dimensional vibrational imaging by coherent anti-Stokes Raman scattering," *Phys. Rev. Lett.* **82**, 4142–4145 (1999).
13. J. Cheng, Y. K. Jia, G. Zheng, and X. S. Xie, "Laser-scanning coherent anti-Stokes Raman scattering microscopy and applications to cell biology," *Biophys. J.* **83**, 502–509 (2002).
14. E. O. Potma, W. P. de Boeij, P. J. M. van Haastert, and D. A. Wiersma, "Real-time visualization of intracellular hydrodynamics in single living cells," *Proc. Natl. Acad. Sci. U.S.A.* **98**, 1577–1582 (2001).
15. N. Dudovich, D. Oron, and Y. Silberberg, "Single-pulse coherently controlled nonlinear Raman spectroscopy and microscopy," *Nature* **418**, 512–514 (2002).
16. D. Oron and Y. Silberberg, "Third-harmonic generation with cylindrical Gaussian beams," *J. Opt. Soc. Am. B* **21**, 1964–1968 (2004).
17. R. Boyd, *Nonlinear Optics* (Academic, 1992).
18. J.-X. Cheng and X. S. Xie, "Green's function formulation for third-harmonic generation microscopy," *J. Opt. Soc. Am. B* **19**, 1604–1609 (2002).
19. A. M. Weiner, "Femtosecond pulse shaping using spatial light modulators," *Rev. Sci. Instrum.* **71**, 1929–1960 (2000).